

# Land-use legacies and tree species richness affect short-term resilience in reforested areas of the world's largest refugee camp

Faqrul Islam Chowdhury<sup>a,b,c,\*</sup>, Rezaul Hasan Bhuiyan<sup>d,e</sup>, Josep Maria Espelta<sup>a,b</sup>, Víctor Resco de Dios<sup>f,g</sup>, Tasnima Dilshad<sup>c</sup>, Md. Riyadul Haque<sup>e</sup>, Md. Aman Ullah Aman<sup>c</sup>, Francisco Lloret<sup>a,b</sup>

<sup>a</sup> Universitat Autònoma de Barcelona, Bellaterra (Cerdanyola del Vallès), Catalonia E08193, Spain

<sup>b</sup> CREAf, Bellaterra, Catalonia E08193, Spain

<sup>c</sup> Institute of Forestry and Environmental Sciences, University of Chittagong, Chattogram, Bangladesh

<sup>d</sup> Department of Natural Resources, University of Twente, 7514 AE Enschede, Netherlands

<sup>e</sup> Department of Environmental Science and Disaster Management, Noakhali Science and Technology University, Noakhali, Bangladesh

<sup>f</sup> Department of Forest and Agricultural Science and Engineering, Universitat de Lleida, Lleida E25198, Spain

<sup>g</sup> JRU CTFC-AGROTECNIO-CERCA Center, Lleida E25198, Spain

## ARTICLE INFO

### Keywords:

Enhanced vegetation index  
Forced migration  
Land-use changes  
Reforestation  
Relative resilience  
Restoration

## ABSTRACT

Forced migration has recently emerged as a deforestation driver in refugee camps, while reforestation offers a solution to restore these degraded ecosystems. The arrival of one million refugees to Kutupalong camp (south-eastern Bangladesh), the world's largest refugee camp, led to significant forest losses after migrant influx, where restoration efforts were subsequently undertaken. However, the effectiveness of these reforestation efforts, and their consequences on vegetation health, remain largely unexplored. This study evaluated the recovery and resilience of reforestation by analyzing enhanced vegetation index (EVI) dynamics, considering the legacy effects of previous land-use systems (natural forest- vs. plantation-legacy plots), tree species richness, and local topography as co-factors. Reforested areas in Kutupalong showed a resilience value of 0.64, indicating that they are still in the recovery phase. Higher recovery was observed in reforested plots that were forests before migrant influx, while pre-deforestation EVI values were associated with higher resilience in plantation-legacy plots. Forest-legacy plots with higher tree species richness exhibited higher recovery probably due to complementarity benefits, driven by resource sharing among multiple tree species. Yet, monospecific plots with *Acacia auriculiformis* in plantation-legacy plots exhibited higher resilience, likely due to growth related traits. Additionally, undisturbed topsoil, especially in lower elevations, could further enhance recovery and resilience. Findings of this study recommend monospecific *A. auriculiformis* plantations where admixtures are not feasible, while considering the legacy effects of previous land-uses and implementing soil restoration strategies. These measures potentially improve vegetation health, enhance the local environment, and ultimately contribute to better living conditions to camp inhabitants.

## 1. Introduction

Global acceleration of deforestation, especially in tropical countries is causing detrimental effects on climate, biodiversity, and essential ecosystem services (Giam, 2017; IPBES, 2019). Historically, forest losses in tropical countries have been closely linked to anthropogenic activity, such as land-use changes for commodity production (Curtis et al., 2018). Recently, forced migration has also contributed to deforestation locally

(e.g., in refugee camps), as a result of the housing and fuelwood needs for camp residents (Bernard et al., 2022; Hassan et al., 2018; Salemi, 2021). The role of forced migration as a global driver of deforestation, and its impacts on biodiversity are significantly smaller than deforestation induced by other anthropogenic causes. However, deforestation and forest degradation in the refugee camps still pose substantial environmental threats to its inhabitants, including local increases in land surface temperature, landslides, and losses of biodiversity and forest

\* Corresponding author at: Universitat Autònoma de Barcelona, Bellaterra (Cerdanyola del Vallès), Catalonia E08193, Spain.

E-mail addresses: [FaqrulIslam.Chowdhury@autonoma.cat](mailto:FaqrulIslam.Chowdhury@autonoma.cat), [faqrul@cu.ac.bd](mailto:faqrul@cu.ac.bd) (F.I. Chowdhury).

<https://doi.org/10.1016/j.ecoleng.2025.107612>

Received 21 August 2024; Received in revised form 1 March 2025; Accepted 12 March 2025

Available online 22 March 2025

0925-8574/© 2025 The Authors. Published by Elsevier B.V. This is an open access article under the CC BY license (<http://creativecommons.org/licenses/by/4.0/>).

goods (Ahmed et al., 2020; Rashid et al., 2021; Sarkar et al., 2023). Addressing these environmental challenges is crucial, aligning with the mandate of the United Nations High Commissioner for Refugees (UNHCR) to ensure proper living conditions for displaced populations, including access to a healthy environment (UNHCR, 2005). Effective reforestation efforts could represent a potential action in mitigating these environmental risks by offering a nature-based solution (Thapa et al., 2024), thus enhancing the well-being of individuals living in a refugee camp.

Reforestation measures could reinstate and restore critical ecosystem services and provide resilience to degraded forest landscapes. Specifically, effective reforestation efforts contribute to stabilize soil quality, provide habitat for biodiversity, and ameliorate ecological functioning (Cunningham et al., 2015; Jourgholami et al., 2019; Veldkamp et al., 2020; Wang et al., 2022). These, in turn, can ensure the supply of goods and services from the forested landscape to the refugees. Several management decisions during reforestation activities can help to achieve such goals. Reforestation in degraded ecosystems with a forest land-use legacy (that is, where natural forests represented the prevailing vegetation before degradation) has shown high recovery and, therefore, providing high resilience, while land-use intensification has been linked with opposite effects (Meli et al., 2017). Additionally, several ecological factors likely contribute to the success of reforestation and related resilience outcomes. Species-specific traits, such as resprouting capacity and water-use efficiency, often perform better in water-limited

conditions (Zeppel et al., 2015). Similarly, higher tree species richness and diversity promote biomass productivity through complementary benefits and niche partitioning and could facilitate quick recovery (Liang et al., 2016; Tatsumi, 2020). Yet, at higher tree species richness, this positive biodiversity-productivity relationship saturates, and it may even induce tree mortality due to overyielding (Liang et al., 2016; Searle et al., 2022). In addition to management and species selection, topographical features such as elevation can also influence the recovery of tropical forests. For instance, higher elevation sites often show slower recovery than lower-elevation sites, likely as a result of temperature inhibitions at high elevations (Yu and Gao, 2020). Overall, current research has identified several drivers of vegetation resilience, but the complex interaction of these factors in recovering vegetation and habitats in tropical forests degraded by refugee settlement remains largely unexplored.

Resilience can be understood as the capacity of a disturbed ecosystem to recover its pre-disturbance ecosystem properties (i.e., engineering resilience; sensu Pimm, 1984; see Gunderson, 2000). So, the comparison of the current state to the pre-disturbance and the disturbed situation provides a measure of resilience and recovery, respectively (Lloret et al., 2011). Measuring resilience requires identifying the value of an ecological characteristic (i.e., a system variable, e.g., the operational resilience framework or ORF, see Lloret et al., 2024), such as, tree growth, taxonomic diversity, and/or functional diversity before the disturbance (i.e. the reference state) and its value during, and after the

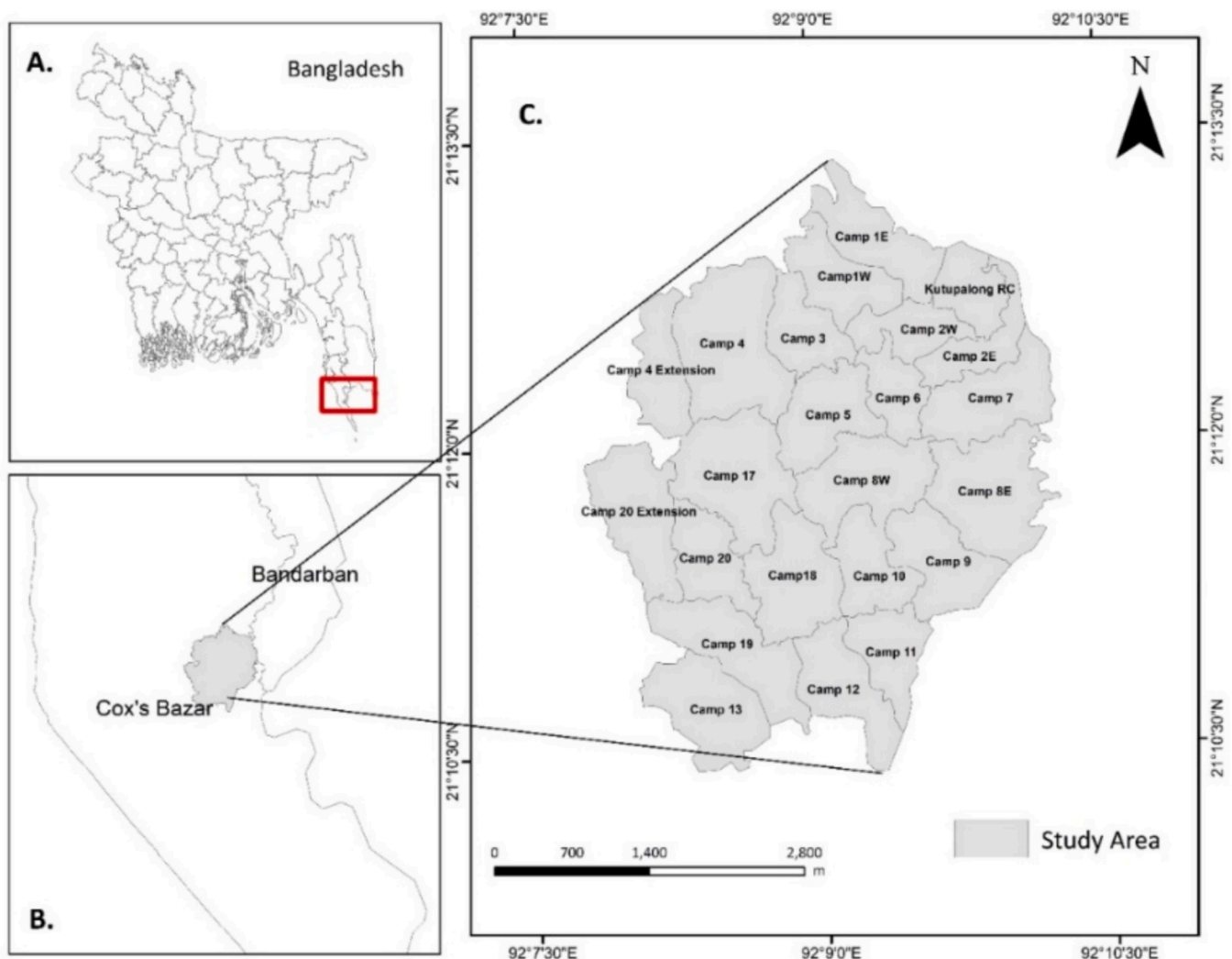


Fig. 1. Location map showing the refugee camps in Kutupalong (southeastern Bangladesh) along with the sub-camps.

disturbance episodes (Lloret et al., 2011). But the evaluation of the resilience of these ecological properties is challenging because forest inventory-based sampling of the pre-disturbance state is often lacking. In this context, remote sensing-related vegetation indices can provide an option to monitor vegetation dynamics on large spatial and temporal scales (Vicente-Serrano et al., 2016). Vegetation indices such as normalized difference vegetation index (NDVI) and enhanced vegetation index (EVI) are increasingly being implemented to detect the changes of primary productivity, and to evaluate the resilience to drought, wildfire, pest outbreaks, and extreme climatic events (Blanco-Rodríguez and Espelta, 2022; Hossain and Li, 2021; Karim et al., 2023; Palmero-Iniesta et al., 2021; Zheng et al., 2016). Thus, NDVI and/or EVI can be used to estimate the recovery and resilience of vegetation cover and health after suffering deforestation and subsequent reforestation.

This study assessed the success of reforestation at the Kutupalong refugee camp (southeastern Bangladesh; Fig. 1), the world's largest refugee camp with 1454 ha of land, where around one million inhabitants currently live (UNHCR, 2024). The Rohingya people, a Muslim ethnic minority group in Myanmar, were forcibly migrated in 2017 from Myanmar and settled here (Hasan et al., 2021). Before camp establishment, the area historically sustained a dense forested landscape with small amount of forest and plantation losses (Fig. S1), and provided habitat for many endangered species (such as the iconic Asian Elephant, *Elephas maximus*) in several surrounding protected areas, including the Teknaf Wildlife Sanctuary, Inani National Park, and Himchari National Park. However, the sudden movement of 750,000 Rohingya refugees in August 2017 resulted in significant forest loss within these protected areas (Fig. S1), with previous natural and plantation forests areas converted into houses and infrastructures for refugees (Hassan et al., 2018). Heavy machinery was also introduced to flatten the landscape and allow house establishment. This led to a reduction of the forest goods and services required by the population (e.g., firewood) and an increase in the vulnerability to flash floods and landslides during the monsoon season (Ahmed et al., 2020; Hasan et al., 2021; Kamal et al., 2023). This dramatic land-use change also posed several risks for local biodiversity, resulting from the blocking of wildlife corridors, disruption of ecosystem functions and the onset of human-elephant conflicts (Mahamud et al., 2022). With the goal of protecting camp inhabitants from environmental threats (e.g., landslides) and restoring some ecosystem functions, stakeholders working in the camp have collaborated to reforest open spaces within camp boundaries, started in 2018 and continued until 2019 during the first phase (Mahamud et al., 2022).

However, existing research are lacking any information on the success of reforestation in Kutupalong, despite the importance of being the world's largest refugee camp (but see Mahmood et al., 2025). Here, the effectiveness of reforestation was evaluated through EVI dynamics over the years since the start of reforestation in 2018 in order to elucidate how land-use legacies (i.e., previous forested vs. plantation forest land-use), tree species richness (i.e., planted during reforestation campaign), and topography influence the short-term recovery and the resilience of reforested areas in Kutupalong (southeastern Bangladesh). Specifically, the study hypothesized that (i) forest-legacy sites with multiple tree species will recover faster and exhibit better resilience than plantation-legacy sites due to soil legacy effects and tree functional complementarity, and (ii) sites with undisturbed soil during the land flattening and settlement establishment will exhibit higher recovery and resilience due to better soil structure and less nutrient depletion. Assessing recovery and resilience and its potential drivers can inform on the success of reforestation efforts in deforested Kutupalong refugee camp and provide data-based policy guidelines for future reforestation activities in similar tropical forests, particularly in those within refugee camp settings, in order to provide better refugee management and environmental restoration.

## 2. Methods

### 2.1. Study area and reforestation efforts

The Kutupalong refugee camp is in Cox's Bazar (21.2126°N to 92.1634°E), Bangladesh. The camp sites and surroundings have a sub-tropical climate with an annual rainfall of 4000 mm and average mean annual temperatures of 26.1 °C.

Reforestation efforts following the 2017's deforestation started after the monsoon season of 2018 and ended in late 2019. Although the tree plantation campaign continued after 2019, this study only considered the 2018–2019 period, because it provides enough time for an initial assessment of recovery and resilience to deforestation in the reforested areas. Multiple tree species were planted in most of the sites in both years, and mulching was used to protect the soil and moisture. However, the choice of tree species has evolved over time. For instance, the Bangladesh Forest Department only encouraged native tree species for plantation during 2019, while up until 2018, non-native tree species were also allowed in the reforestation sites (Mahamud et al., 2022). Normally, all sites followed similar management practices, including two weeding events the first year after planting, and daily watering to planted saplings for the first six months.

### 2.2. Sampling design

#### 2.2.1. Land-use and land cover (LULC) classification

In order to select the sampling plots and to determine the type of land-use legacies, land-use and land cover (LULC) classification maps of Kutupalong camp were created for 2017, 2018, and 2020 using Random Forest algorithm in Google Earth Engine (Gorelick et al., 2017; Table S1; Fig. S2). The LULC classes considered for the classification purpose were natural forest (forest hereafter), degraded forest, plantation forest (plantation hereafter), settlement, agriculture, and water body. Using the GEE platform, Sentinel-2 Level-1C images were downloaded and only selected those with less than 5 % cloudiness for January 2017, 2018, and 2020 to define the LULC classes. Spectral bands 2–8, 8a, and 11–12 of Sentinel-2 were used for LULC classification. Additionally, NDVI was derived using the red (Band 4) and near-infrared (Band 8) bands and incorporated into the feature layer to enhance classification accuracy. High-resolution Google Earth images were used to generate at least 30 training points for each land-use class, which were distributed randomly throughout the study area. The training data was then imported into GEE as a feature collection table, and the Random Forest algorithm was used to generate LULC classifications. Accuracy assessments for LULC image of each year were performed using a confusion matrix in GEE to validate and assess the accuracy of the classification. The overall accuracy for 2017, 2018, and 2020 were 96 %, 85 % and 92 % respectively, while the Kappa coefficients were 0.95, 0.82, and 0.89, respectively (Table S1).

#### 2.2.2. Identification of land-use legacy area and selection of sampling plots

A four-step procedure was adopted to identify land-use legacies and to select the sampling plots for assessing vegetation resilience and its factors. First, the 2017's LULC classification was used to identify land-use legacies before the deforestation event. Forest and plantation LULC classes were considered as forest land-use-legacy (hereafter, forest-legacy) and plantation land-use-legacy (hereafter, plantation-legacy), respectively. Second, the image of 2018 was used to select deforested areas, while the images from the 2020's were utilized to detect the area being reforested. Third, the areas that were either forest or plantation in 2017, deforested in 2018, and reforested by 2019 (i.e., 2020's map) were selected. These polygons were then chosen for additional sampling (Fig. S3A). Finally, 188 points were randomly selected by using "random point selection" features from ESRI's ArcMap (Fig. S3B), which were later used in field sampling. Among them, 103 plots belong to the forest-legacy type, while 85 plots to plantation-

legacies (Fig. S3B-D).

### 2.3. Field sampling camping to identify tree species and topographical features

During 2023, field sampling was conducted at the aforementioned 188 points by establishing  $10 \times 10 \text{ m}^2$  plots to identify the planted tree species. Overall, tree saplings from 17 species were identified across all sampling plots (Table S2). During reforestation, the planted tree saplings were similar in age (i.e., 1–2 years old) and size (i.e., collar diameter of 2–2.5 cm, and height of <130 cm). Collar diameter of the tree saplings were measured to compute basal area. Furthermore, to quantify the dominance of individual species, the important value index (IVI) between forest-legacy and plantation-legacy plots was computed, according to Curtis and McIntosh (1951). The IVI (in %) can be expressed as:

$$IVI = \frac{RDe + RF + RDo}{3} \quad (1)$$

where, RDe is the relative density of the species (RD = density of a species/total density of all species  $\times 100$ ), RF is the relative frequency of the species (RF = frequency of a species/total frequency of all species  $\times 100$ ) and RDo is the relative dominance of the species (RDo = basal area of a species/total basal area of all species  $\times 100$ ). Here, density was calculated as the ratio between the total number of individuals of a species in all plots, divided by the total number of plots. Frequency was computed as the ratio between the total number of plots where a species is present and the total number of plots. Dominance was calculated as the proportion of the basal area of a species and the total basal area of all species in all plots.

In addition to tree species, several topographical features in each plot, including elevation, aspect and slope were also collected during field sampling. This is because the camp area underwent a high degree of topographical changes to prepare housing and infrastructure settlement. Suunto Clinometer and compass (PM-5/360 PC. Vantaa, Finland: Suunto) were used for measuring slope, and aspect, while a digital elevation model (DEM; source USGS Earth Explorer; see USGS, 2024) was utilized to determine each plot's elevation.

### 2.4. Quantifying resilience indices

Resilience is usually assessed by examining the influence of a disturbance (e.g., drought, pest attack, deforestation, etc.) on ecological parameters (e.g., tree growth, basal area, vegetation indices, etc.). This study considered the 2017's deforestation event in the refugee camp as a disturbance, and the enhanced vegetation index (EVI) as an ecological feature (i.e., indicator of vegetation biomass). EVI is extensively used as an indicator of forest productivity as it is related to leaf biomass (Vicente-Serrano et al., 2016).

#### 2.4.1. Quantifying EVI as the ecological property of resilience

To calculate resilience indices, the median of EVI values for the 188 plots were collected at different time points: (i) before the arrival of the refugees, representing the pre-deforestation period (January 2017); (ii) during camp establishment or immediately after the deforestation (January 2018); and (iii) after reforestation (January of each 2020, 2021, 2022, and 2023 year; see Figs. S4, S5 for details). EVI images were derived from Sentinel-2 and obtained through GEE as:

$$EVI = \frac{2.5 (NIR - RED)}{NIR + 6 RED - 7.5 BLUE + 1} \quad (2)$$

where, NIR, RED and BLUE indicates near infrared band, red band, and blue band, respectively.

#### 2.4.2. Computing EVI-based resilience indices

The resilience indices for each of the 188 plots were computed by

comparing changes in EVI before the deforestation, immediately after deforestation, and the post deforestation periods. Following Lloret et al. (2011), recovery and resilience were estimated for each year for the 2020–2023 period. Resistance was not computed because in the study system the alteration caused by deforestation was so intense that it could not be well discriminated through the camp.

Recovery was computed as the ratio of post-deforestation EVI (Post-EVI) values (i.e., EVI median values in January for each year in 2020–2023) to EVI values immediately following deforestation (Defor-EVI; EVI median values in January 2018). Meanwhile, resilience was calculated as the ratio of Post-EVI to EVI values prior to the disturbance period (PreEVI; median EVI values in January 2017):

$$\text{Recovery} = \frac{\text{PostEVI}}{\text{DeforEVI}} \quad (3)$$

$$\text{Resilience} = \frac{\text{PostEVI}}{\text{PreEVI}} \quad (4)$$

The relative resilience, which is used to identify the resilience weighted by the damage incurred during the disturbance, was also derived by following Lloret et al. (2011):

$$\text{Relative resilience} = \frac{\text{PostEVI} - \text{DeforEVI}}{\text{PreEVI}} \quad (5)$$

### 2.5. Statistical analyses

Linear mixed models (LMMs) were applied to determine the effects of land-use legacy, year, tree species richness, sapling density and topography on EVI resilience indices. In the LMMs, the values of EVI recovery, resilience, and relative resilience were used as separate dependent variables, while year, land-use legacy (forest- vs. plantation-legacy), tree species richness, sapling density, and topographical features (aspect, slope, and elevation) were included as explanatory variables. The interaction-terms: year  $\times$  land-use legacy, land-use legacy  $\times$  tree species richness, land-use legacy  $\times$  sapling density, land-use legacy  $\times$  aspect, land-use legacy  $\times$  slope, and land-use legacy  $\times$  elevation were also included as explanatory variables in the full model of each resilience indices. In each LMM, “plot location” was treated as a random effect to eliminate possible autocorrelation (i.e. repeated measures sampling). Additionally, to determine the variation between forest and plantation-legacy of EVI in each year, and the degree of variation in recovery, resilience, and relative resilience across years (2020–2023 period), post-hoc tests with the Tukey's HSD was performed after checking the appropriate assumptions (i.e., after confirming the significance of  $p$ -value in associated ANOVA).

All statistical analyses and plotting were performed in R (version 4.3.2; R Core Team, 2024). The “lmer” function from the “lme4” library was utilized to run the LMMs (Bates et al., 2024; R Core Team, 2024). Continuous explanatory variables in LMMs were scaled to standardize the data as they were of very different magnitude. Then, the backward model selection strategies were applied, based on the model with the lowest AIC values, using a threshold of 2 (Burnham et al., 2011). The residuals of all models were tested for autocorrelation using the ACF test from “stats” package and normality assumptions were checked with residual plots (R Core Team, 2024). R libraries such as “sjPlots” and “ggplot2” were used for graphing (Lüdtke et al., 2024; Wickham et al., 2024).

## 3. Results

### 3.1. Land-use and land cover (LULC) changes between 2017 and 2020

The LULC classes in Kutupalong camp showed dramatic changes between 2017 and 2020 (Table 1, Fig. S2). The forest and plantation areas showed an 80 % and an 89 % reduction between 2017 (pre-



**Table 1**

Land-use and land cover (LULC) changes for 2017–2020 in the Kutupalong camp. Here, forest and plantation denote to natural forest and plantation forest, respectively, while agriculture indicates agricultural land.

LULC classes	2017	2018	2020
	Area (ha)		
Forest	595	119	132
Degraded forest	22	31	32
Plantation	451	51	115
Agriculture	331	445	251
Water body	24	31	13
Settlement	31	776	909

deforestation) and 2018 (immediately after deforestation), respectively. This was because of rapid increases in settlement (96 %) and agricultural (26 %) lands, respectively, at the same time (Table 1). However, until the end of 2019 (i.e., 2020's LULC), there was a 10 % and a 56 % increase in the areas covered by forest and plantation LULC after the post-reforestation. This forest and plantation growth occurred at the expense of agricultural lands, as their extent was reduced by 44 %. However, during 2018–2020 period, settlement areas increased by 12 % (Table 1). Water bodies and degraded forests comprised small areas in the Kutupalong camp (3 % of total areas in 2017), but showed a 31 % reduction and a 46 % increase, respectively, during 2017–2020 period (Table 1).

### 3.2. Status of tree species composition and topography in reforested sites

There were 17 and 15 different tree species saplings in forest-legacy and plantation-legacy plots, respectively (Tables S2, S3). Mean tree species richness per plot were  $1.9 (\pm 0.05 \text{ se})$  and  $2.1 (\pm 0.04 \text{ se})$  in forest-legacy and plantation-legacy plots, respectively, while the mean densities (plot sapling/ha) were 2834 and 2937, respectively (Table S4).

The differences in species dominance (i.e., important value index or IVI) between land-use legacies was apparent (Table S3). In forest-legacy plots, *Gmelina arborea* was dominant (IVI = 11 %) followed by *Ficus carica* (IVI = 9.8 %), *Brownlowia elata* (IVI = 8.5 %), *Protium serratum* (IVI = 8 %), and *Trema orientalis* (IVI = 7.5 %) (see details in Table S4). Meanwhile, *Acacia auriculiformis* (IVI = 22.6) was dominant in plantation-legacy plots, followed by *Ficus carica* (IVI = 13.5 %), *Lagerstroemia speciosa* (IVI = 11.4 %), *Grewia nervosa* (IVI = 9.4 %), and *Gmelina arborea* (IVI = 9.1 %; see details in Table S3). Among topographical features, elevation and slope were similar in forest and plantation-legacy plots (i.e., elevation were 19 m and 18 m, and slope were 1.7 % and 2 %, respectively (Table S4). Vegetation and topographical features (i.e., tree species richness, density, elevation, slope, and aspect) in the studied plots were weakly correlated among them (Fig. S6).

### 3.3. Dynamics of the enhanced vegetation index (EVI) and drivers of resilience

EVI was significantly higher in forest-legacy plots than in plantation-legacy ones before camp establishment (i.e., in the January of 2017). After the deforestation episodes, EVI was significantly higher in plantation-legacy plots in 2018 and remained higher in 2020 (i.e., immediately after reforestation). However, EVI of forest-legacy plots became significantly higher across 2021–2023 period (Fig. 2).

Regarding resilience indices, significant changes in EVI recovery were observed across years (Fig. 3A; Tables 2, S5; significance of the year terms with  $p < 0.001$  in the ANOVA, see more: Table S6). EVI recovery first declined from 2.1 in 2020 to 1.9 in 2021. EVI recovery then increased to 2.1 and 2.2 during 2022 and 2023, respectively (Fig. 3A; Table S7). Importantly, EVI recovery was significantly higher in forest-legacy plots than in plantation-legacy ones (Tables 2, S5). The significant interaction between land-use legacy and year on recovery showed a

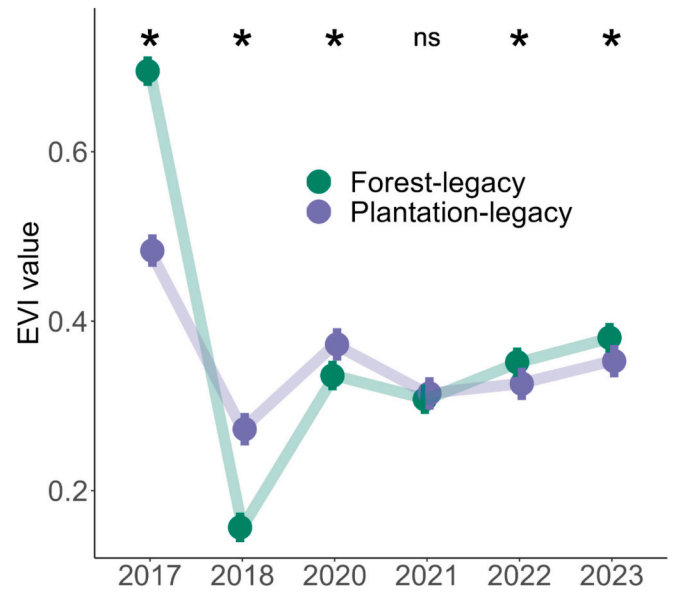


**Fig. 2.** Enhanced vegetation index (EVI) values between land-use legacies (forest- vs. plantation-legacy) across 2017–2023. EVI value in 2017 corresponds to the pre-deforestation condition, while 2018 and 2020–2023 corresponds to the situation immediately after deforestation and after reforestation, respectively. The asterisk and “ns” indicate significant differences according to Tukey’s HSD at 95 % CI or non-significance, respectively, between forest- and plantation-legacy plots.

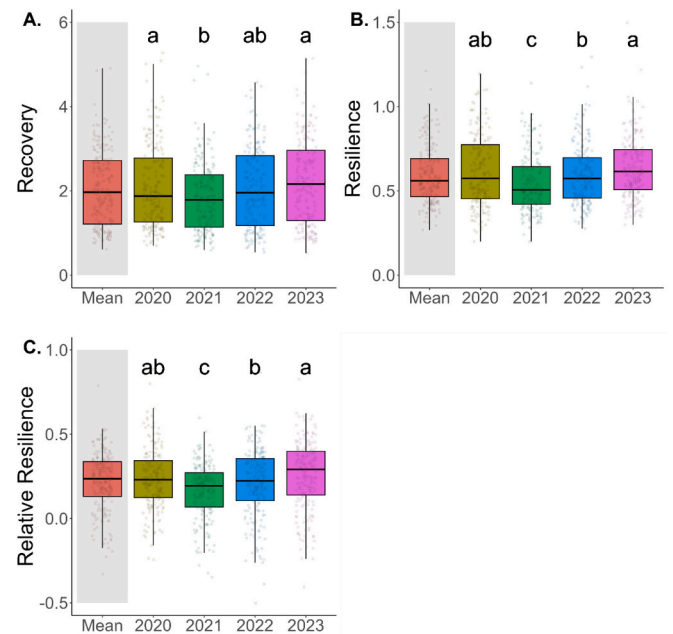


**Fig. 3.** Boxplots of (A) recovery, (B) resilience, and (C) relative resilience of enhanced vegetation index (EVI) across 2020–2023 period. Overall mean values of recovery, resilience, and relative resilience shaded in grey, and their data points are also shown. a, b, and c denote significant differences of Tukey’s HSD test at 95 % CI. See Tables S7, S10 and S13 for further details.

larger recovery in forest-legacy plots, relative to plantation-legacy plots across 2020–2023 period (Fig. 4A, Tables 2, S5). Furthermore, the significant interaction between tree species richness and land-use legacies indicated that the higher EVI recovery in forest-legacy plots, relative to plantation-legacy ones, increased with higher tree species richness

**Table 2**

Estimates of linear mixed models (LMMs) to determine the effect of land-use legacies (LUL; forest-legacy and plantation-legacy), tree species richness, and elevation on (A) recovery, (B) resilience, and (C) relative resilience in reforested areas of the Kutupalong refugee camp (southeastern Bangladesh). See Tables S5, S8 and S11 for further details.

Predictors	Estimates		
	(A) Recovery	(B) Resilience	(C) Relative resilience
Year [2021]	−0.22 ***	−0.04 ***	−0.04 ***
Year [2022]	0.11 *	0.02 *	0.02 *
Year [2023]	0.30 ***	0.06 ***	0.06 ***
LUL [Plantation-legacy]	−0.46 ***	0.26 ***	−0.03
Tree species richness	0.21 **	0.06 ***	0.05 ***
Elevation	−0.13	−0.01	0.00
Aspect		0.00	0.06 ***
Year [2021]: LUL [Plantation-legacy]	−0.11	−0.08 ***	−0.08 ***
Year [2022]: LUL [Plantation-legacy]	−0.34 ***	−0.12 ***	−0.12 ***
Year [2023]: LUL [Plantation-legacy]	−0.39 ***	−0.11 ***	−0.11 ***
LUL [Plantation-legacy]: Tree species richness	−0.41 **	−0.05 *	−0.09 ***
LUL [Plantation-legacy]: Elevation	0.47 ***	−0.06 **	0.09 ***

\*  $p < 0.05$ .

\*\*  $p < 0.01$ .

\*\*\*  $p < 0.001$ .

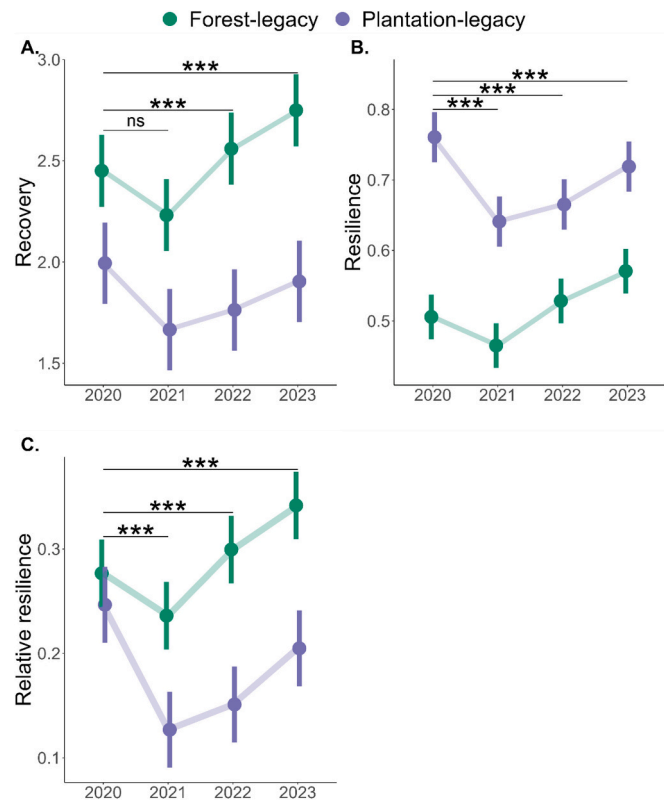


**Fig. 4.** Interaction effects of land-use legacy (forest- vs. plantation-legacy) and year (2020–2023) for (A) recovery, (B) resilience, and (C) relative resilience of enhanced vegetation index (EVI). Asterisks indicate the significance level of  $p$ -values (\*:  $p < 0.05$ , \*\*:  $p < 0.01$ , \*\*\*:  $p < 0.001$ ) and ns denotes to non-significance.

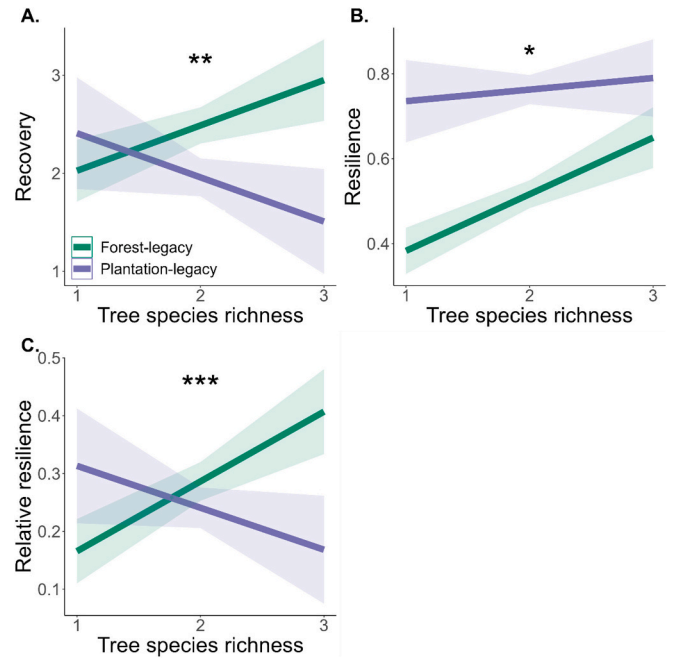


**Fig. 5.** Interaction effect of land-use legacy (forest- vs. plantation-legacy) and tree species richness (number per plot) for (A) recovery, (B) resilience, and (C) relative resilience of enhanced vegetation index (EVI). Asterisks indicate the significance level (\*:  $p < 0.05$ , \*\*:  $p < 0.01$ , \*\*\*:  $p < 0.001$ ). The envelop around the effect lines denotes the 95 % confidence interval.

(Fig. 5A, Tables 2, S5). Finally, a larger recovery of forest-legacy plots, relative to plantation-legacy ones, appeared in the plots at lower elevation (Fig. 6A, Table S5).

Regarding resilience, EVI also significantly varied across years (Fig. 3B; Tables 2, S8; significance of the year terms with  $p < 0.001$  in the

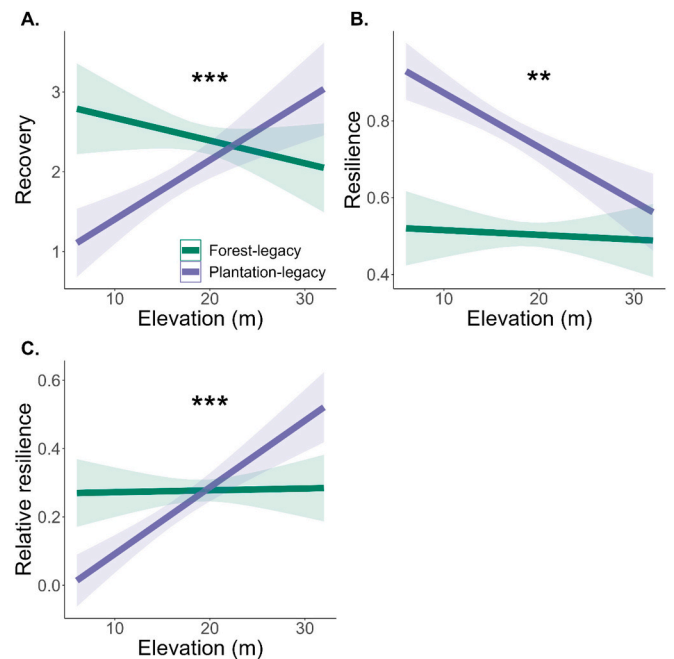


**Fig. 6.** Interaction effects of land-use legacy (forest- vs. plantation-legacy) and elevation (meter) for (A) recovery, (B) resilience, and (C) relative resilience of enhanced vegetation index (EVI). Asterisks indicate the significance level (\*:  $p < 0.05$ , \*\*:  $p < 0.01$ , \*\*\*:  $p < 0.001$ ). The envelop around the effect lines denotes the 95 % confidence interval.

ANOVA, see more: Table S9). EVI resilience first declined from 0.62 in 2020 to 0.54 in 2021, but then increased to 0.59 and 0.64 in years 2022 and 2023, respectively (Fig. 3B; S10). Contrary to recovery, resilience was significantly higher across plantation legacy plots (Tables 2, S8). Similarly, the significant interaction between land-use legacy and year on resilience showed that the higher resilience in plantation-legacy plots compared to forest-legacy ones occurred in the 2020–2023 period (Fig. 4B, Tables 2, S8). Interestingly, the significant interactions of land-use legacy with tree species richness and elevation indicated that higher EVI resilience in plantation-legacy plots occurred under lower tree richness and lower elevation, respectively (Figs. 5B, 6B; Tables 2, S8).

EVI relative resilience also significantly varied across the 2020–2022 period (Fig. 3C; Tables 2, S11; significance of the year terms with  $p < 0.001$  in the ANOVA, see more: Table S12). Relative resilience first declined from 0.24 in 2020 to 0.16 in 2021, and then increased to 0.21 and 0.26 in 2022 and 2023, respectively (Fig. 3C; S13). EVI relative resilience was significantly higher in forest-legacy plots than in plantation-legacy ones across the 2021–2023 period (Fig. 4C; Tables 2, S11). Similar to EVI recovery, relative resilience was higher in forest-legacy than plantation-legacy in the plots with higher tree species richness and at lower elevation (Figs. 5C, 6C; Tables 2, S11).

The random terms (i.e., plot locations) increased the conditional  $R^2$  by 70 %, 49 %, and 59 % in recovery, resilience, and relative resilience LMMs, respectively (Tables S5, S8 and S11).

#### 4. Discussion

The study reveals recovery capacity, in terms of EVI, in the reforested areas of Kutupalong refugee camps that experienced severe deforestation. Although resilience, relative to the pre-disturbance values, was not complete in the short period of observations, full recovery is expected to occur relatively soon, i.e. in next 12 years, assuming that the rate of recovery of measured between 2021 and 2023 is maintained. Interestingly, findings of this study suggest that reforestation areas exert strong legacy effects due to previous land-uses, which in turn determine recovery and resilience: forest-legacy plots exhibited higher recovery, while plantation-legacy plots showed higher resilience. This suggests that different mechanisms drive recovery and resilience in the study area. Tree species richness also affected EVI resilience in both forest and plantation-legacy plots. More specifically, the higher recovery in forest-legacy plots was accentuated by higher tree richness, likely due to functional complementarity effects of tree species (Liang et al., 2016). In turn, the plantation-legacy plots showed higher resilience at lower tree species richness, likely due to the functional characteristics of planted species. Higher growth rate of dominant tree species in plantation-legacy plots (i.e., *A. auriculiformis*, a fast-growing tree species, with IVI = 22.6 % in plantation-legacy plots vs. IVI = 4.5 % in forest-legacy ones; see more in Table S3) could potentially determine such differences. Additionally, topographical characteristics (i.e., elevation in this case) also contribute to explain EVI recovery and resilience. In the case of elevation, intact topsoil at lower elevations (that is, areas that were not affected during infrastructure construction) may further enhance the recovery and resilience in forest-legacy and plantation-legacy plots, respectively.

##### 4.1. Temporal changes in vegetation cover and resilience indices

After reforestation, forest cover increased in the beginning of 2020, owing to the reforestation efforts in the camp. Furthermore, the potential soil seed and bud banks in the deforested areas could also provide sources for propagule regeneration and resprouting (Ma et al., 2021). Combinedly, reforestation and potential seed and bud banks could increase forest cover in the Kutupalong refugee camp within a short period. Forest cover loss because of deforestation and post-reforestation forest gain in the study area aligned with findings from previous studies (Hassan et al., 2018, 2023). Ultimately, this increase in forest cover

recovered some of the ecosystem services in the Kutupalong camp (Mahmood et al., 2024, 2025).

A gradual increase in EVI recovery and resilience was observed across the years, after a small decline in 2021. Initial management (e.g., watering, mulching, patch weeding, etc.; see methods for details) supported the survival and growth of the saplings (Mahamud et al., 2022). However, at the end of the intervention period, saplings became more vulnerable to water limitations and heat stress (Rashid et al., 2021), which could have resulted sapling defoliation or even mortality. These losses might contribute to the decline of the resilience indices in 2021. Subsequently, as saplings acclimated, they experienced a progressive recovery in 2021 and following years.

##### 4.2. Effects of land-use legacy, tree species richness, and elevation on resilience indices

This study found a strong legacy effects, especially in the plots that were forests before camp settlement. Reforestation performed in forest-legacy plots could have benefited from higher soil organic matter and nutrient availability, relative to plantation forests (Chowdhury et al., 2022; De Schrijver et al., 2012; Freschet et al., 2014). Additionally, restoration of degraded forests in the tropics increases enzymatic activities and provides faster soil carbon and nutrient cycling, which in turn enhanced plant productivity and could contribute to a faster recovery (Feng et al., 2019). Here pre-deforestation EVI was higher in the forest-legacy plots compared to the plantation-legacy ones, indicating a higher plant cover in forest-legacy plots, which ultimately promoted higher EVI recovery. Furthermore, at higher tree species richness, recovery and resilience showed an increasing trend in forest-legacy plots likely due to tree diversity's complementary effect on productivity (Liang et al., 2016). Indeed, high tree species diversity or admixtures has been commonly suggested as a key contributor to enhance forest productivity and recovery (Chazdon et al., 2023; Liu et al., 2019). Additionally, during housing construction, hilly areas in the camp were flattened (Ahmed et al., 2020; Mahamud et al., 2022). Thus, forest-legacy plots at lower elevations showed higher recovery, at least partly because the topsoil in these plots might be less affected by camp settlement than the plots at higher elevation.

Plantation-legacy plots showed higher EVI resilience than forest-legacy plots, indicating that resilience might not only stem from differences in EVI recovery but also from differences in pre-disturbance and post-reforestation states. Specifically, the resilience values referred to here reflect two different pre-disturbance states: one corresponding to plantation-legacy plots, which had smaller vegetation cover or relatively younger trees than natural forests, resulting in lower pre-deforestation EVI in these plots. Additionally, the decrease in EVI in plantation-legacy plots was lower than in forest-legacy plots during deforestation. Thereby, despite lower EVI recovery, plantation-legacy plots showed higher values of EVI resilience. Interestingly, differences in tree species functional traits may also partly explain the higher EVI resilience in the plantation-legacy plots with low species richness (e.g., monospecific stands). Plantation-legacy plots in the study locations were dominated by *A. auriculiformis*, a fast-growing tree species that is popular in plantation programs in Bangladesh. It has greater site adaptability and relatively high growth rates (Islam et al., 2013). Specifically, this tree species has a wide tolerance spectrum in terms of soil pH (4.5–8.5), high water-use-efficiency, and can grow in degraded lands with low nutrient concentrations; thereby, maintaining high growth rates even under stressed conditions (Chowdhury and Ishiguri, 2009; Rahman et al., 2017). Such high growth rates could lead to the observed faster increase of EVI to pre-disturbance levels (i.e., higher short-term resilience) in plantation-legacy plots. But this mechanism was not effective enough to provide faster EVI recovery. So, at low species richness level, EVI recovery and resilience responded differently, thus pinpointing the needs of further research on the role of functional traits of *A. auriculiformis* in long-term resilience process.

## 5. Conclusion and policy implications

Reforestation plays a crucial role in restoring vegetation cover after the deforestation caused by the establishment of the Kutupalong refugee camp. The reforested areas in the camps are undergoing gradual recovery, influenced by the legacy effects from previous land-use systems, the plantation techniques (i.e., admixture vs. monospecific plantation), and local topography. Forest- and plantation-legacies have been shown to play a critical role in enhancing vegetation recovery and resilience. Higher tree species richness further strengthened recovery, underscoring the importance of maintaining tree biodiversity. Meanwhile, monospecific tree plantations with fast-growing and hardy tree species like *A. auriculiformis* could attain short-term resilience. Thereby, if admixture plantation is not feasible due to resource or logistical constraints, monospecific plantation with *A. auriculiformis* could be alternative silvicultural approach, especially to overcome nutrient and water limitations. Additionally, soil restoration, particularly in upper-elevation areas that underwent topsoil degradation, could accelerate the recovery of vegetation health and cover. The example of reforestation efforts in the Kutupalong refugee camp demonstrate the potential of reforestation to promote vegetation recovery and resilience within camp environment. This might eventually enhance the ecological conditions of the camp sites and potentially improve other ecosystem services, such as quality air provision, soil erosion control, and access to resources to camp inhabitants.

## CRedit authorship contribution statement

**Faqrul Islam Chowdhury:** Writing – review & editing, Writing – original draft, Visualization, Methodology, Funding acquisition, Formal analysis, Data curation, Conceptualization. **Rezaul Hasan Bhuiyan:** Writing – review & editing, Visualization, Data curation. **Josep Maria Espelta:** Writing – review & editing, Supervision, Methodology. **Víctor Resco de Dios:** Writing – review & editing. **Taslima Dilshad:** Writing – review & editing, Project administration, Investigation. **Md. Riyadul Haque:** Writing – review & editing, Investigation, Data curation. **Md. Aman Ullah Aman:** Writing – review & editing, Investigation, Data curation. **Francisco Lloret:** Writing – review & editing, Supervision, Methodology.

## Declaration of competing interest

The authors declare that they have no known competing financial interests or personal relationships that could have appeared to influence the work reported in this paper.

## Acknowledgement

The work was supported by the Research and Publication Cell of Chittagong University (Bangladesh). The authors also express their gratitude to the “la Caixa” Foundation (ID 100010434, INPhINIT fellowship code: LCF/BQ/DI21/11860064), UNEP/UNESCO/BMUV Training Program – TUD Dresden University of Technology – CIPSEM – Innovation Fellowship (SC83), and AGAUR, Generalitat of Catalonia (2021 SGR 00849).

## Appendix A. Supplementary data

Supplementary data to this article can be found online at <https://doi.org/10.1016/j.ecoleng.2025.107612>.

## Data availability

Data will be made available on request.

## References

- Ahmed, B., Rahman, M.S., Sammonds, P., Islam, R., Uddin, K., 2020. Application of geospatial technologies in developing a dynamic landslide early warning system in a humanitarian context: the Rohingya refugee crisis in Cox's Bazar, Bangladesh. *Geomat. Nat. Hazards Risk* 11, 446–468. <https://doi.org/10.1080/19475705.2020.1730988>.
- Bates, D., Maechler, M., Bolker, B., Walker, S., Christensen, R.H.B., Singmann, H., Dai, B., Scheipl, F., Grothendieck, G., Green, P., Krivitsky, P.N., Bauer, A., Fox, J., Tanaka, E., Jagan, M., 2024. lme4: Linear Mixed-Effects Models using “Eigen” and S4. <https://github.com/lme4/lme4/> (date accessed: 01/08/2024).
- Bernard, B., Aron, M., Loy, T., Muhamud, N.W., Benard, S., 2022. The impact of refugee settlements on land use changes and vegetation degradation in West Nile Sub-region, Uganda. *Geocarto Int.* 37, 16–34. <https://doi.org/10.1080/10106049.2019.1704073>.
- Blanco-Rodríguez, M.Á., Espelta, J.M., 2022. Tree species composition and management influence short-term resilience to defoliation by *Lymantria dispar* L. in oak forests. *For. Ecol. Manag.* 520. <https://doi.org/10.1016/j.foreco.2022.120399>.
- Burnham, K.P., Anderson, D.R., Huyvaert, K.P., 2011. AIC model selection and multimodel inference in behavioral ecology: some background, observations, and comparisons. *Behav. Ecol. Sociobiol.* <https://doi.org/10.1007/s00265-010-1029-6>.
- Chazdon, R.L., Norden, N., Colwell, R.K., Chao, A., 2023. Monitoring recovery of tree diversity during tropical forest restoration: lessons from long-term trajectories of natural regeneration. *Philos. Trans. R. Soc. B Biol. Sci.* 378. <https://doi.org/10.1098/rstb.2021.0069>.
- Chowdhury, M.Q., Ishiguri, F., 2009. Wood property variation in *Acacia auriculiformis* growing in Bangladesh. *Wood Fiber Sci.* 41, 1–7.
- Chowdhury, F.I., Barua, I., Chowdhury, A.I., Resco de Dios, V., Alam, M.S., 2022. Agroforestry shows higher potential than reforestation for soil restoration after slash-and-burn: a case study from Bangladesh. *Geol. Ecol. Landsc.* 6, 48–54. <https://doi.org/10.1080/24749508.2020.1743528>.
- Cunningham, S.C., Cavanaugh, T.R., Mac Nally, R., Paul, K.I., Baker, P.J., Beringer, J., Thomson, J.R., Thompson, R.M., 2015. Reforestation with native mixed-species plantings in a temperate continental climate effectively sequesters and stabilizes carbon within decades. *Glob. Chang. Biol.* 21, 1552–1566. <https://doi.org/10.1111/gcb.12746>.
- Curtis, J.T., McIntosh, R.P., 1951. An upland forest continuum in the prairie-forest border region of Wisconsin. *Ecology* 32, 476–496. <https://doi.org/10.2307/1931725>.
- Curtis, P.G., Slay, C.M., Harris, N.L., Tyukavina, A., Hansen, M.C., 2018. Classifying drivers of global forest loss. *Science* 1979. <https://doi.org/10.1126/science.aau3445>.
- De Schrijver, A., De Frenne, P., Staelens, J., Verstraeten, G., Muys, B., Vesterdal, L., Wuyts, K., van Nevel, L., Schelfhout, S., De Neve, S., Verheyen, K., 2012. Tree species traits cause divergence in soil acidification during four decades of postagricultural forest development. *Glob. Chang. Biol.* 18, 1127–1140. <https://doi.org/10.1111/j.1365-2486.2011.02572.x>.
- Feng, C., Ma, Yuhua, Jin, X., Wang, Z., Ma, Yan, Fu, S., Chen, H.Y.H., 2019. Soil enzyme activities increase following restoration of degraded subtropical forests. *Geoderma* 351, 180–187. <https://doi.org/10.1016/j.geoderma.2019.05.006>.
- Freschet, G.T., Ostlund, L., Kichenin, E., Wardle, D.A., 2014. Aboveground and belowground legacies of native Sami land use on boreal forest in northern Sweden 100 years after abandonment. *Ecology* 95, 963–977. <https://doi.org/10.1890/13-0824.1>.
- Giam, X., 2017. Global biodiversity loss from tropical deforestation. *Proc. Natl. Acad. Sci. USA*. <https://doi.org/10.1073/pnas.1706264114>.
- Gorelick, N., Hancher, M., Dixon, M., Ilyushchenko, S., Thau, D., Moore, R., 2017. Google Earth Engine: planetary-scale geospatial analysis for everyone. *Remote Sens. Environ.* 202, 18–27. <https://doi.org/10.1016/j.rse.2017.06.031>.
- Gunderson, L.H., 2000. Ecological resilience - in theory and application. *Annu. Rev. Ecol. Evol. Syst.* 31, 425–439.
- Hasan, M.E., Zhang, L., Mahmood, R., Guo, H., Li, G., 2021. Modeling of forest ecosystem degradation due to anthropogenic stress: the case of rohingya influx into the Cox's bazar–Teknaf peninsula of Bangladesh. *Environments* 8. <https://doi.org/10.3390/environments8110121>.
- Hassan, M.M., Smith, A.C., Walker, K., Rahman, M.K., Southworth, J., 2018. Rohingya refugee crisis and forest cover change in Teknaf, Bangladesh. *Remote Sens.* 10. <https://doi.org/10.3390/rs10050689>.
- Hassan, M.M., Duveneck, M., Southworth, J., 2023. The role of the refugee crises in driving forest cover change and fragmentation in Teknaf, Bangladesh. *Ecol. Inform.* 74. <https://doi.org/10.1016/j.ecoinf.2022.101966>.
- Hossain, M.L., Li, J., 2021. NDVI-based vegetation dynamics and its resistance and resilience to different intensities of climatic events. *Glob. Ecol. Conserv.* 30. <https://doi.org/10.1016/j.gecco.2021.e01768>.
- IPBES, 2019. The Global Assessment Report of the Intergovernmental Science-Policy Platform on Biodiversity and Ecosystem Services.
- Islam, S.S., Islam, M.S., Hossain, Md.A.T., Alam, Z., 2013. Optimal rotation interval of akashmoni (*acacia auriculiformis*) plantations in Bangladesh. *Kasetsart J.* 34, 181–190.
- Jourgholami, M., Ghassemi, T., Labelle, E.R., 2019. Soil physio-chemical and biological indicators to evaluate the restoration of compacted soil following reforestation. *Ecol. Indic.* 101, 102–110. <https://doi.org/10.1016/j.ecolind.2019.01.009>.
- Kamal, A.S.M.M., Hossain, F., Ahmed, B., Rahman, M.Z., Sammonds, P., 2023. Assessing the effectiveness of landslide slope stability by analysing structural mitigation measures and community risk perception. *Nat. Hazards* 117, 2393–2418. <https://doi.org/10.1007/s11069-023-05947-6>.



- Karim, M.R., Mukul, S.A., Zahir, R.B., Saimun, S.R., Arfin-Khan, M.A.S., 2023. The role of protected areas co-management in enhancing resistance and resilience of deciduous forest ecosystem to extreme climatic events in Bangladesh. *J. Environ. Manag.* 326. <https://doi.org/10.1016/j.jenvman.2022.116800>.
- Liang, J., Crowther, T.W., Picard, N., Wiser, S., Zhou, M., Alberti, G., Schulze, E.D., McGuire, A.D., Bozzato, F., Pretzsch, H., De-Miguel, S., Paquette, A., Hérault, B., Scherer-Lorenzen, M., Barrett, C.B., Glick, H.B., Hengeveld, G.M., Nabuurs, G.J., Pfautsch, S., Viana, H., Vibrans, A.C., Ammer, C., Schall, P., Verbilya, D., Tchebakova, N., Fischer, M., Watson, J.V., Chen, H.Y.H., Lei, X., Schelhaas, M.J., Lu, H., Gianelle, D., Parfenova, E.I., Salas, C., Lee, E., Lee, B., Kim, H.S., Brulheide, H., Coomes, D.A., Piotta, D., Sunderland, T., Schmid, B., Gourlet-Fleury, S., Sonké, B., Tavan, R., Zhu, J., Brandl, S., Vayreda, J., Kitahara, F., Searle, E.B., Neldner, V.J., Ngugi, M.R., Baraloto, C., Frizzera, L., Balazy, R., Oleksyn, J., Zawila-Niedzwiecki, T., Bouriaud, O., Bussotti, F., Finér, L., Jaroszewicz, B., Jucker, T., Valladares, F., Jagodzinski, A.M., Peri, P.L., Gonmadje, C., Marthy, W., O'Brien, T., Martin, E.H., Marshall, A.R., Rovero, F., Bitarho, R., Niklaus, P.A., Alvarez-Loayza, P., Chamuya, N., Valencia, R., Mortier, F., Wortel, V., Engone-Obiang, N.L., Ferreira, L.V., Odeke, D.E., Vasquez, R. M., Lewis, S.L., Reich, P.B., 2016. Positive biodiversity-productivity relationship predominant in global forests. *Science* 354. <https://doi.org/10.1126/science.1250057>.
- Liu, Xiaofei, Garcia-Ulloa, J., Cornioley, T., Liu, Xuehua, Wang, Z., Garcia, C., 2019. Main ecological drivers of woody plant species richness recovery in secondary forests in China. *Sci. Rep.* 9. <https://doi.org/10.1038/s41598-018-35963-7>.
- Lloret, F., Keeling, E.G., Sala, A., 2011. Components of tree resilience: effects of successive low-growth episodes in old ponderosa pine forests. *Oikos* 120, 1909–1920. <https://doi.org/10.1111/j.1600-0706.2011.19372.x>.
- Lloret, F., Hurtado, P., Espelta, J.M., Jaime, L., Nikinmaa, L., Lindner, M., Martínez-Vilalta, J., 2024. ORF, an operational framework to measure resilience in social-ecological systems: the forest case study. *Sustain. Sci.* <https://doi.org/10.1007/s11625-024-01518-1>.
- Lüdtke, D., Bartel, A., Schwemmer, C., Powell, C., Djalovski, A., Titz, J., 2024. sjPlot: Data Visualization for Statistics in Social Science. <https://strengexjacke.github.io/sjPlot/> (date accessed: 01/08/2024).
- Ma, M., Collins, S.L., Ratajczak, Z., Du, G., 2021. Soil seed banks, alternative stable state theory, and ecosystem resilience. *Bioscience*. <https://doi.org/10.1093/biosci/biab011>.
- Mahamud, R., Jalal, R., Donegan, E., Arif, T., Kumar, M., De Gaetano, M., Kabir, H., Hemry, M., 2022. Restoring Degraded Land in Rohingya Refugee Camps in Cox's Bazar, Bangladesh.
- Mahmood, H., Saha, C., Saha, S., Tanvir, M.S.S.I., Sakal, S.N.H., 2024. Shifts in soil quality from degradation to early phase of forest restoration: evidence from Rohingya refugee camps, Cox's Bazar, Bangladesh. *Trees For. People* 18. <https://doi.org/10.1016/j.tfp.2024.100701>.
- Mahmood, H., Saha, C., Saha, S., 2025. Tracking forest recovery: early biomass and carbon stock monitoring in the Rohingya Refugee camps, Cox's Bazar, Bangladesh. *Environ. Chall.* 18. <https://doi.org/10.1016/j.envc.2024.101063>.
- Meli, P., Holl, K.D., Benayas, J.M.R., Jones, H.P., Jones, P.C., Montoya, D., Mateos, D.M., 2017. A global review of past land use, climate, and active vs. passive restoration effects on forest recovery. *PLoS One*. <https://doi.org/10.1371/journal.pone.0171368>.
- Palmero-Iniesta, M., Pino, J., Pesquer, L., Espelta, J.M., 2021. Recent forest area increase in Europe: expanding and regenerating forests differ in their regional patterns, drivers and productivity trends. *Eur. J. For. Res.* 140, 793–805. <https://doi.org/10.1007/s10342-021-01366-z>.
- Pimm, S.L., 1984. The complexity and stability of ecosystems. *Nature*. <https://doi.org/10.1038/307321a0>.
- R Core Team, 2024. R: A Language and Environment for Statistical Computing. Vienna, Austria. <https://www.R-project.org/> (date accessed: 01/08/2024).
- Rahman, M.M., Rahma, M.A., Miah, M.G., Saha, S.R., Karim, M.A., Mostofa, M.G., 2017. Mechanistic insight into salt tolerance of *Acacia auriculiformis*: the importance of ion selectivity, osmoprotection, tissue tolerance, and Na<sup>+</sup> exclusion. *Front. Plant Sci.* 8. <https://doi.org/10.3389/fpls.2017.00155>.
- Rashid, K.J., Hoque, M.A., Esha, T.A., Rahman, M.A., Paul, A., 2021. Spatiotemporal changes of vegetation and land surface temperature in the refugee camps and its surrounding areas of Bangladesh after the Rohingya influx from Myanmar. *Environ. Dev. Sustain.* 23, 3562–3577. <https://doi.org/10.1007/s10668-020-00733-x>.
- Salemi, C., 2021. Refugee camps and deforestation in Sub-Saharan Africa. *J. Dev. Econ.* 152. <https://doi.org/10.1016/j.jdeveco.2021.102682>.
- Sarkar, S.K., Saroar, M.M., Chakraborty, T., 2023. Cost of ecosystem service value due to Rohingya refugee influx in Bangladesh. *Disaster Med. Public Health Prep.* 17. <https://doi.org/10.1017/dmp.2022.125>.
- Searle, E.B., Chen, H., Paquette, H.Y., David Lindenmayer, A., Member Alan Hastings, B., 2022. Higher tree diversity is linked to higher tree mortality. *PNAS*. <https://doi.org/10.1073/pnas>.
- Tatsumi, S., 2020. Tree diversity effects on forest productivity increase through time because of spatial partitioning. *For. Ecosyst.* 7. <https://doi.org/10.1186/s40663-020-00238-z>.
- Thapa, P.S., Daimaru, H., Yanai, S., 2024. Analyzing vegetation recovery and erosion status after a large landslide at Mt. Hakusan, Central Japan. *Ecol. Eng.* 198. <https://doi.org/10.1016/j.ecoleng.2023.107144>.
- UNHCR, 2005. UNHCR: Environmental Guidelines. <https://www.unhcr.org/media/unhcr-environmental-guidelines> (date accessed: 01/08/2024).
- UNHCR, 2024. Rohingya Emergency [WWW Document]. <https://www.unhcr.org/emergencies/rohingya-emergency> (date accessed: 01/08/2024).
- USGS, 2024. Shuttle Radar Topography Mission (SRTM). <https://earthexplorer.usgs.gov/>.
- Veldkamp, E., Schmidt, M., Powers, J.S., Corre, M.D., 2020. Deforestation and reforestation impacts on soils in the tropics. *Nat. Rev. Earth Environ.* <https://doi.org/10.1038/s43017-020-0091-5>.
- Vicente-Serrano, S.M., Camarero, J.J., Olano, J.M., Martín-Hernández, N., Peña-Gallardo, M., Tomás-Burguera, M., Gazol, A., Azorin-Molina, C., Bhuyan, U., El Kenawy, A., 2016. Diverse relationships between forest growth and the normalized difference vegetation index at a global scale. *Remote Sens. Environ.* 187, 14–29. <https://doi.org/10.1016/j.rse.2016.10.001>.
- Wang, C., Zhang, W., Li, X., Wu, J., 2022. A global meta-analysis of the impacts of tree plantations on biodiversity. *Glob. Ecol. Biogeogr.* 31, 576–587. <https://doi.org/10.1111/geb.13440>.
- Wickham, H., Chang, W., Henry, L., Pedersen, T.L., Takahashi, K., Wilke, C., Woo, K., Yutani, H., Dunnington, D., van den Brand, T., Posit, P., 2024. ggplot2: Create Elegant Data Visualisations Using the Grammar of Graphics. <https://ggplot2.tidyverse.org/> (date accessed: 01/08/2024).
- Yu, M., Gao, Q., 2020. Topography, drainage capability, and legacy of drought differentiate tropical ecosystem response to and recovery from major hurricanes. *Environ. Res. Lett.* 15. <https://doi.org/10.1088/1748-9326/abae2c>.
- Zeppel, M.J.B., Harrison, S.P., Adams, H.D., Kelley, D.I., Li, G., Tissue, D.T., Dawson, T. E., Fensham, R., Medlyn, B.E., Palmer, A., West, A.G., McDowell, N.G., 2015. Drought and resprouting plants. *New Phytol.* 206, 583–589. <https://doi.org/10.1111/nph.13205>.
- Zheng, Z., Zeng, Y., Li, S., Huang, W., 2016. A new burn severity index based on land surface temperature and enhanced vegetation index. *Int. J. Appl. Earth Obs. Geoinf.* 45, 84–94. <https://doi.org/10.1016/j.jag.2015.11.002>.